

Cite this: *Mater. Adv.*, 2022,
3, 4289

pH-Controlled forms of 1-amino-1-hydrazino-2,2-dinitroethylene (HFOX): selective reactivity of amine and hydrazinyl groups with aldehydes or ketones†

Ajay Kumar Chinnam, ^a Richard J. Staples ^b and Jean'ne M. Shreeve ^{*a}

1-Amino-1-hydrazino-2,2-dinitroethylene (HFOX) is a potential reactive intermediate for a new class of energetic materials. Now we describe its condensation with various carbonyl compounds in the presence of acidic and basic catalysts. Condensation of HFOX with α -diones and β -diones gives products of much interest. α -Diones undergo cyclization in the presence of base to form six-membered ring products, while β -diones cyclize to five-membered ring products in the presence of acid. One of the exciting reactions is the formation of ammonium (5,6-dimethyl-1,2,4-triazin-3-yl)dinitromethanide salt, **5c**, which was isolated by using aqueous ammonia as a nucleophilic base. All new compounds were fully characterized by advanced spectroscopic techniques. The structures of **5**, **5c**, **5e**, **9**, **11**, and **12a** are supported by single crystal X-ray diffraction analysis. Most of the new six membered ring compounds have good thermostabilities (>200 °C), while the fluorinated five membered ring compound, **12b**, has the highest density of 2.04 g cm⁻³ at 25 °C. Heats of formation and detonation properties were calculated by using Gaussian 03 and EXPLO5 software programs. Nearly all new compounds have very good detonation properties, especially, triazine salts, **5e** ($D_v = 7513$ m s⁻¹; $P = 24.45$ GPa), and **5f** ($D_v = 7948$ m s⁻¹; $P = 26.27$ GPa) as well as azide derivative **11** ($D_v = 8166$ m s⁻¹; $P = 25.48$ GPa), which are superior to TNT ($D_v = 6824$ m s⁻¹; $P = 19.40$ GPa). These findings provide a new perspective for the synthesis of novel high performing energetic materials.

Received 17th March 2022,
Accepted 11th April 2022

DOI: 10.1039/d2ma00307d

rsc.li/materials-advances

Introduction

1,1-Diamino-2,2-dinitroethylene (FOX-7) is an efficient and insensitive explosive with excellent thermostability and detonation performance comparable with RDX (1,3,5-trinitroperhydro-1,3,5-triazine).¹ It was first synthesized by Latypov, and in 1998 its crystal structure was determined by Östmark.² FOX-7 is a perfect example of a “push–pull ethylene” with a highly polarized carbon–carbon double bond. With its strong electron-withdrawing and electron-donating groups, FOX-7 has attracted significant attention from researchers worldwide.³ Many studies have been pursued on the synthesis, thermal behavior, and explosive performance of FOX-7.⁴ Included among its very attractive properties are high thermostability and insensitivity which arise from the extensive hydrogen bonding between the *gem*-diamino and dinitro groups of FOX-7.

Over the years, many successful attempts have been made to derivative FOX-7.⁵ One of the interesting examples is the nucleophilic substitution of FOX-7 with hydrazine to form 1-amino-1-hydrazino-2,2-dinitroethylene (HFOX, **1**). It is one of the robust and high-performing explosive intermediates with structural features similar to FOX-7. Because of the adjacent amino and hydrazine functionalities in **1**, it is highly reactive or spontaneously decomposes or is extremely dangerous.⁶ Both compounds, FOX-7 and **1**, have poor solubility in common organic solvents. They are amphoteric in nature exhibiting a variety of tautomers and resonance structures which can be reacted with bases or acids.^{7,8} For example, HFOX can form correspondingly the protonated (i) and anionic (ii) forms when reacted with acid and base (Fig. 1).⁷ Both the ionic forms are highly reactive intermediates and result in stable products upon reaction with carbonyl compounds. However, only limited studies on the selectivity of these resonance forms have been utilized for the construction of high-performing materials.^{9–11}

For the past several years, our group has engaged in studies leading to the understanding of the reactivity of FOX-7 and **1** in an effort to expand their chemistry. So far, several strategies have been developed for 1-based high-performing materials.^{12–21}

^a Department of Chemistry, University of Idaho, Moscow, Idaho, 83844-2343, USA.

E-mail: jshreeve@uidaho.edu

^b Department of Chemistry, Michigan State University East Lansing, MI, 48824, USA† Electronic supplementary information (ESI) available. CCDC 2154055–2154059, 1975378 and 1975379. For ESI and crystallographic data in CIF or other electronic format see DOI: <https://doi.org/10.1039/d2ma00307d>

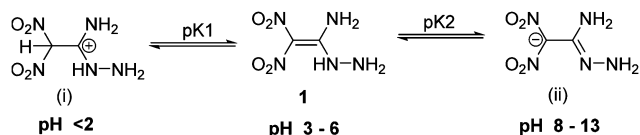


Fig. 1 Different forms of HFOX, **1** under varying pH conditions.

Halogenated derivatives of FOX-7 and **1** are the most attractive towards high energy density materials. In general, halo dinitro methane groups improve the density and oxygen balance, resulting in potentially highly hypergolic oxidizers, which could react with typical rocket fuels. A series of hypergolic oxidizers were achieved by reacting stable derivatives of FOX-7 and **1** with hypochlorite.^{14,15} Another simple strategy for energetic 1,2,4-triazoles is exemplified by reacting **1** with ethyl 3-ethoxy-3-iminopropanoate hydrochloride.^{18,19} A simple strategy for anion- and cation-based energetic salts is shown by reaction of **1** with bases or acids.⁷ Due to its amphoteric nature, **1** gave two different condensed products when it was reacted with glyoxal. With the protonated form of HFOX (i), only the hydrazinyl group participated in condensation with glyoxal.¹⁵ Whereas with the anionic form of HFOX (ii), both amine and hydrazinyl groups participated in the reaction with glyoxal.¹⁷

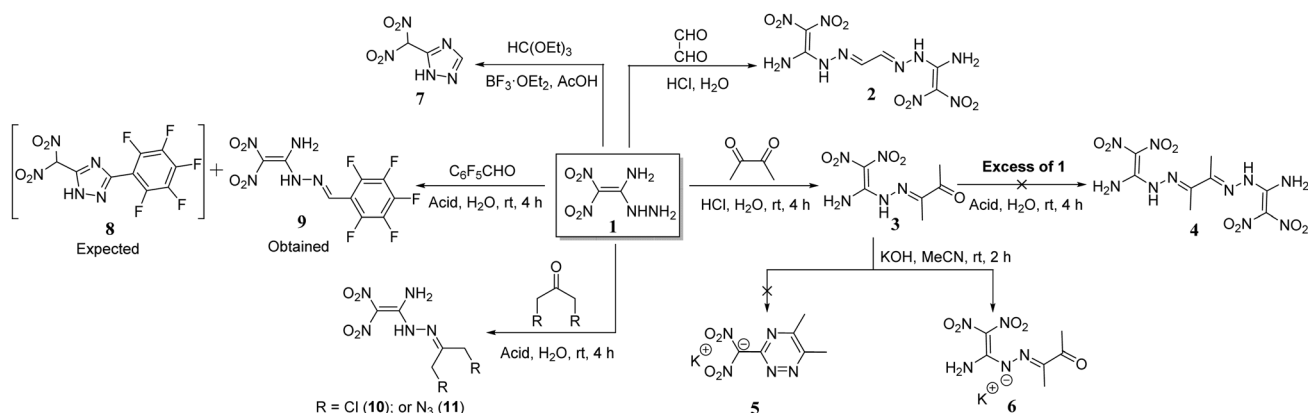
Extending our interest in the chemistry of **1**, we have synthesized several new compounds by reacting it with carbonyls under acidic and basic reaction conditions. Dicarboxyls give very interesting products when reacted with **1**. α -Dione (butane-2,3-dione) reacted in the presence of base to give six-membered products, while β -dione (pentane-2,4-dione) reacted with acid to form five-membered products. One of the exciting reactions is the formation of ammonium salt, **5c**, which was isolated by condensation of **1** with butane-2,3-dione with aqueous ammonia as a base. All new compounds were fully characterized using multinuclear NMR (¹H, ¹³C, ¹⁹F), and elemental analysis, which reveals the selected reactivity of **1** with carbonyls. Thermostabilities and theoretical properties of all new compounds were investigated for practical applications as energetic materials.

Results and discussion

Synthesis

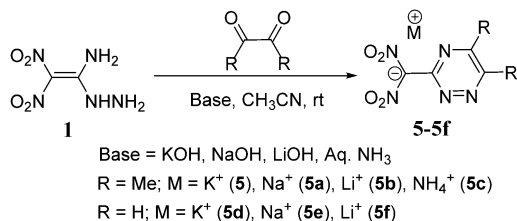
The reaction of **1** with glyoxal in the presence of acidic medium leads to the formation of the dimerized product **2**.¹⁵ But the reaction of **1** with butane-2,3-dione in the acidic solution gave only the mono condensed product, **3**. No dimerized product **4** was formed in the reaction of **3** with excess of **1**. When reacted with aqueous potassium hydroxide in acetonitrile, it gave the potassium salt **6**, but no cyclized triazine salt **5** was formed. Earlier, when compound **1** was reacted with triethyl orthoformate the 1,2,4-triazole derivative **7** was obtained.²² Similarly, we reacted **1** with 2,3,4,5,6-pentafluorobenzaldehyde in order to form the triazole product **8**, but rather, the mono condensed product **9** was observed in quantitative yields. The structures of **6** and **9** are supported by ¹H, ¹³C NMR, and elemental analysis (ESI⁺). In addition, we reacted **1** with symmetrical ketones such as 1,3-dichloroacetone, and 1,3-diazoacetone to give the respective condensed products **10** and **11** in quantitative yields (Scheme 1). These reactions under basic conditions led to the formation of an anionic salt of **1**.

The amine and hydrazinyl groups of **1** reacted with butane-2,3-dione in the presence of potassium hydroxide to give 1,2,4-triazine salt, **5**. Along with butane-2,3-dione, glyoxal was also used as the source of α -carbonyl and the formation of 1,2,4-triazine salts was examined using various metal hydroxides and aqueous ammonia as bases (Scheme 2). Compound **1** and carbonyl compounds were dissolved in acetonitrile, and a metal hydroxide or aqueous ammonia (3 equivalents) was added in a minimum amount of water at room temperature. After stirring at room temperature for 2 hours, solid products, **5–5f**, were isolated by solvent evaporation. Surprisingly, butane-2,3-dione gave the cyclized derivative of the ammonium salt, **5c** in 90% yield. But the reaction of **1** with glyoxal in aqueous ammonia gave the dimerized derivative **2** due to the high reactivity of glyoxal with hydrazinyl of **1**. Similarly, we have reacted compound **1** with α -diones in the presence of hydroxylamine or hydrazine as a nucleophilic base, but cyclized products or their salts were not isolated.



Scheme 1 Condensation of **1** with carbonyl compounds in acidic medium.



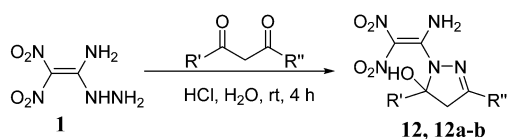


Scheme 2 Condensation of **1** with carbonyl compounds in basic medium.

The reaction of **1** with pentane-2,4-dione in acidic medium gave a five-membered cyclized product **12** with improved yield of 87% (Scheme 3).¹¹ Unexpectedly, both carbonyl groups participated in a condensation reaction with the hydrazinyl group of **1**, and the amino moiety did not participate in the reaction. Similarly, fluorine-substituted diones, 1,1,1-trifluoropentane-2,4-dione and 1,1,1,5,5,5-hexafluoro-2,4-pentanedione reacted with **1** to give cyclized products **12a**, and **12b** in 76% and 64%, respectively.

All new compounds were characterized by ¹H, ¹³C NMR, and IR spectroscopy, and elemental analysis. In the ¹H NMR spectra of **5–5c**, two signals for the methyl protons were observed in the range of 2.50–2.65 ppm, and the NH₄ proton resonances were observed at 7.11 ppm for **5c**, whereas for **5d–f**, two signals of aromatic ring protons were observed between 8.90–9.30 ppm. In the ¹H NMR spectrum of compound **9**, the hydrazinyl NH signal was observed at 13.36 ppm, the NH₂ signal was split into two signals at 10.16 and 9.43 ppm, and the methylene resonance for CH was observed at 8.43 ppm. In the case of compounds **10** and **11**, the hydrazinyl, NH, and NH₂ signals as well as those of CH₂ were observed in the range of 12.46–12.56, 9.32–10.11, 4.26–4.52 ppm, respectively. In the ¹H NMR spectra of **12–12b**, two different signals for NH₂ were found in the range of 8.62–9.61, whereas OH protons were observed between 7.9–10.35 ppm and methylene CH₂ protons were assigned in the range of 1.90–3.70 ppm (ESI[†]).

The structures of **5**, **5c**, **5d**, **9**, **11**, and **12a** were characterized by single crystal X-ray crystallography. All these crystals were obtained without solvent or water molecules in the crystal structure. The triazine salts (**5**, **5c**, and **5d**) were crystallized in mixtures of water and ethanol by slow evaporation at room temperature. Potassium salt **5** crystallizes in two distinct forms (Form I and Form II). The crystallographic data are provided in the (ESI[†]). Form I crystallize in the monoclinic space group *C2/c* and Form II crystallizes in the orthorhombic space group *P2₁2₁2₁*, with calculated densities of 1.743 g cm⁻³ and



Scheme 3 Condensation of **1** with pentane-2,4-dione in acidic medium.

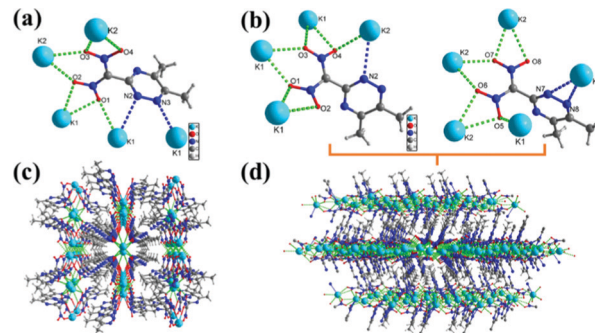


Fig. 2 (a) and (b) Thermal ellipsoid plot (50%) and labeling scheme for Form I of **5** and Form II of **5**. (c) and (d) Ball-and-stick packing diagram for Form I of **5** and Form II of **5** viewed up the *c* axis, and *b* axis, respectively. Dashed lines indicate K–O, and K–N bonding.

1.728 g cm⁻³ at 99.98 K, respectively (Fig. 2(a) and (b)). In both forms of **5**, each unit cell contains eight ((5,6-dimethyl-1,2,4-triazin-3-yl)dinitromethanide) anions, and eight Na ions (*Z* = 8), which have several K–O, and K–N bonds forming a 3D network structure throughout the crystal (Fig. 2(c) and (d)).

The ammonium salt, **5c**, crystallizes in the triclinic space group *P1̄* (*Z* = 2) symmetry with a calculated density of 1.540 g cm⁻³ at 100 K (Fig. 3(a)). All the triazine ring atoms and methyl and dinitromethane carbon atoms are nearly planar with the torsion angles of C1–N1–N2–C2 = –0.77°(16), C4–C1–N3–C3 = 174.61°(9), and N1–N2–C2–C5 = 174.72°(10). The bond distance of C1–C4 = 1.483 (15) Å is slightly shorter compared with C2–C5 = 1.494 (15) Å, and C3–C6 = 1.494(15) Å. Unlike the metal potassium salt **5**, there are extensive hydrogen bond interactions in **5c** between the ammonium cation and the nitro group (5,6-dimethyl-1,2,4-triazin-3-yl)dinitromethanide anion (Fig. 3(b)).

Sodium salt **5e** crystallizes in the orthorhombic space group *Pnma* with a crystal density of 1.931 g cm⁻³ at 100 K (Fig. 4(a)). Each unit cell contains eight dinitro(1,2,4-triazin-3-yl)methanide anions and eight Na ions (*Z* = 8), (ESI[†] Table S1). All the triazine ring atoms are coplanar while the nitro groups are out of the plane. The torsion angles of C5–N5–N6–C6 = 0.0°(0), C8–C5–N7–C7 = 180.0°(0), and C7–C6–N6–Na2 = –180.0°(0). Each Na atom

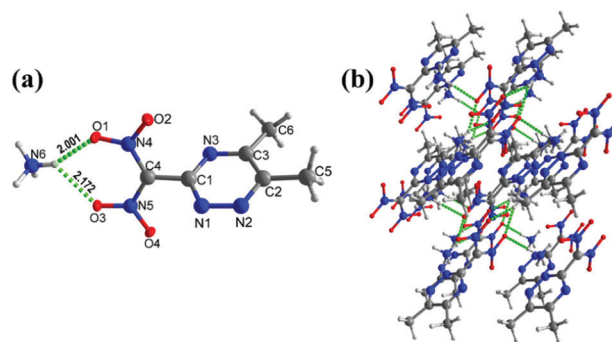


Fig. 3 (a) Thermal ellipsoid plot (50%) and labeling scheme for **5c**. (b) Ball-and-stick packing diagram of **5c** viewed up the *a* axis. Dashed lines indicate strong hydrogen bonds.



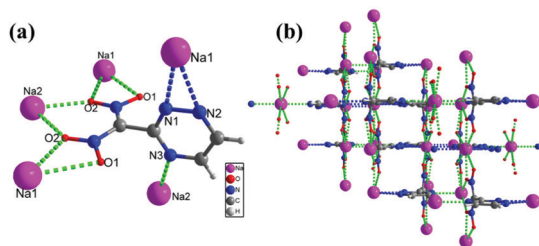


Fig. 4 (a) Thermal ellipsoid plot (50%) and labeling scheme for **5e**. (b) Ball-and-stick packing diagram of **5e** viewed up the *a* axis.

is coordinated with nine bonds to three nitrogen atoms and six oxygen atoms of adjacent triazine anions. The lengths of the Na–O bonds are in the range of 2.476 to 2.794 Å, while the bond lengths of Na–N are between 2.495 to 2.636, respectively. The dinitro(1,2,4-triazin-3-yl)methanide anions also form nine bonds with adjacent Na atoms. The O2 and O3 atoms (NO₂ group) form two bonds with Na1 and Na2, while O1 and O4 form only one bond with Na1 and Na2, respectively. Due to multi coordinate bonds between Na–O, and Na–N in **5e**, forms a 3D framework throughout the crystal (Fig. 4(b)).

Crystals of **9**, **11**, and **12a** were obtained by slow evaporation in methanol at room temperature. Compound **9** crystallizes in the monoclinic space group *P*2₁/*c* with a density of 1.952 g cm⁻³ at 173 K (Fig. 5(a)). The C1=C2 bond length is 1.442 Å in **9** compared with the C=C bond length of 1.456 Å in FOX-7.⁸ In the crystal structure of **9**, the perfluorophenyl and ethylene amine atoms are nearly planar with torsion angles of N2–C3–C4–C9 = 5.1°(3), N1–N2–C3–C4 = -175.07°(13), and N2–N1–C1–N5 = 4.5°(2), respectively. The two nitro groups lie out of plane relative to the amine group and phenyl ring, with torsion angles of O1–N3–C2–C1 = 37.1°(2) and O4–N4–C2–C1 = 11.4°(2), respectively. In addition, the intramolecular and intermolecular hydrogen bonds involving N1–H1···O4, N5–H5A···O1, and N5–H5A···O3 are observed (Fig. 5(b)).

Compound **11** crystallizes in the monoclinic space group *C*2/*c* with a density of 1.669 g cm⁻³ at 172.99 K (Fig. 6(a)). The C4=C5 bond length is 1.433 Å compared with the C=C bond length of 1.456 Å in FOX-7.⁸ In the crystal structure, the atoms of ethylene amine and the hydrazinyl group are nearly planar with torsion angles of N2–N1–C4–N3 = -0.8°(2), N1–N2–C1–C2 = 0.3°(2), and N2–N1–C4–C5 = 179.48°(12), respectively. Both azide groups lie out of the plane with of the ethylene amine and hydrazine moieties. The dinitromethyl group lies out of plane as in compound **9**, with torsion angles of O1–N10–C5–C4 = 14.0°(2)

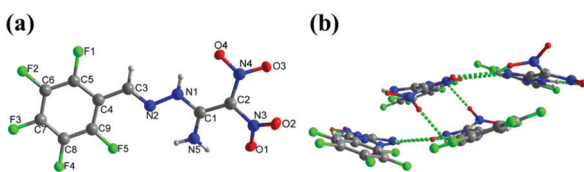


Fig. 5 (a) Thermal ellipsoid plot (50%) and labeling scheme for **9**. (b) Ball-and-stick packing diagram of **9** viewed up the *a* axis. Dashed lines indicate strong hydrogen bonding.

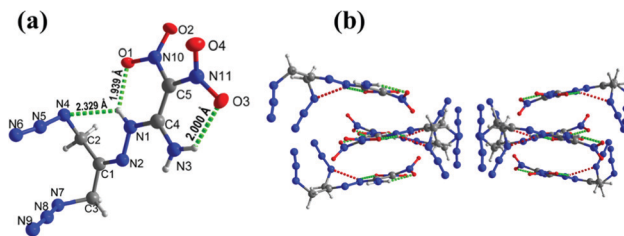


Fig. 6 (a) Thermal ellipsoid plot (50%) and labeling scheme for **11**. (b) Ball-and-stick packing diagram of **11** viewed up the *c* axis. Dashed lines indicate strong hydrogen bonding.

and O3–N11–C5–C4 = 30.0°(2), respectively. In addition, the juxtaposed amino and nitro groups of the ethylene group participate in intra, and intermolecular hydrogen bonds observed in the crystal packing of **9** (Fig. 6(b)).

Compound **12a** crystallizes in the triclinic space group *P*1 with a density of 1.714 g cm⁻³ at 173 K (Fig. 7(a)). The C6=C7 bond length is 1.480 Å in **12a**, which is slightly higher compared with the C=C bond length in **9** and **11**. The five-membered heterocyclic ring and the adjoining amino group are almost coplanar, with torsion angles of C1–N1–C6–N3 = 4.5°(3), and N2–N1–C6–N3 = 173.73°(16), respectively. The dinitromethyl group is nearly perpendicular to both the amine moiety and the five-membered heterocyclic ring with angles of N3–C6–C7–N4 = -93.0°(2), N1–C6–C7–N4 = 86.3°(2), and N1–C6–C7–N5 = -83.7°(2), respectively. In addition, intramolecular hydrogen bonds involving N3–H3B···O3, and N3–H3A···O1 are observed (Fig. 7(b)).

Physicochemical and energetic properties

Thermal stabilities of all new compounds were determined using differential scanning calorimetric (DSC) measurements with a heating rate of 5 °C min⁻¹. All triazine derivatives have good thermostabilities (> 205 °C) except **5c** (171 °C) and **5d** (168 °C). Three pyrazole-based compounds, **12** (156 °C), **12a** (184 °C), and **12b** (171 °C) are more thermally stable than their parent HFOX (124 °C). Compounds **9** and **11** have the lowest decomposition temperatures at 157 °C and 109 °C, respectively. The densities of all new compounds were measured using a gas pycnometer at 25 °C, and the values are between 1.44 g cm⁻³ (**12**) to 2.04 g cm⁻³ (**12b**). Compounds **9** (1.84 g cm⁻³), **5e** (1.89 g cm⁻³), and **12b**

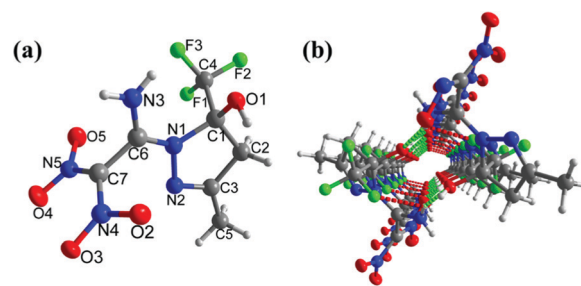


Fig. 7 (a) Thermal ellipsoid plot (50%) and labeling scheme for **12a**. (b) Ball-and-stick packing diagram of **12a** viewed up the *a* axis. Dashed lines indicate strong hydrogen bonding.



Table 1 Energetic properties of new compounds compared with TNT

Comp.	T_d^a [°C]	ρ^b [g cm ⁻³]	ΔH_f^c [kJ mol ⁻¹] /kJ g ⁻¹	D_v^d [m s ⁻¹]	P^e [GPa]	IS^f [J]	FS^g [N]
5	238	1.70	9.1/0.04	6543	15.75	22	>360
5a	260	1.63	90.0/0.38	6501	15.69	25	>360
5b	168	1.58	174.9/0.79	7031	17.95	29	>360
5c	158	1.50	139.1/0.60	7212	17.86	>40	>360
5d^h	270	1.88	104.8/0.57	7252	22.10	4	240
5e	303	1.89	148.5/0.72	7513	24.45	8	360
5f	201	1.75	236.3/1.24	7948	26.27	10	>360
9	157	1.85	-692/-2.02	6976	22.49	>40	>360
11	109	1.63	745/2.61	8166	25.48	12	240
12ⁱ	156	1.44	-226/-0.92	6674	14.77	14	240
12a	184	1.70	-869/-2.90	6937	20.26	27	>360
12b	171	2.04	-1469/-4.16	7173	24.51	>40	>360
TNT^j	300	1.65	-59.3/-0.26	6824	19.40	15	353

^a Decomposition temperature (onset). ^b Density – gas pycnometer at 25 °C. ^c Calculated molar enthalpy of formation. ^d Calculated detonation velocity (Explo5 v6.01). ^e Calculated detonation pressure (Explo5 v6.01). ^f Impact sensitivity. ^g Friction sensitivity. ^h Ref. 17 ⁱ Ref. 11 ^j Ref. 21

(2.04 g cm⁻³) have highest densities. Heats of formation for all new compounds were calculated using the Gaussian 03 suite of programs with isodesmic reactions (ESI[†]).²³ Compound **11** (745 kJ mol⁻¹) possesses a high positive heat of formation relative to the triazine derivatives **5–5e** (between 9.1 to 236.3 kJ mol⁻¹), because of a large number of N–N bonds. In comparison, fluorine-containing compounds and **12a** have relatively negative heats of formation (ΔH_f) due to the presence of many C–F bonds and non-aromatic pyrazoline rings.

Based on the values of experimental densities and calculated heats of formation, the detonation pressure (P) and detonation

velocity (D_v) were calculated using EXPLO5 (version 6.01).²⁴ The calculated detonation pressures (P) range between 14.77 and 26.72 GPa and calculated detonation velocities (D_v) between 6501 and 8166 m s⁻¹. All new compounds have excellent detonation properties and are comparable to TNT ($P = 19.5$ GPa; $D_v = 6881$ m s⁻¹). Impact and friction sensitivities values were obtained using BAM drop hammer and friction tester techniques.²⁵ Most of the new compounds are relatively sensitive to impact and friction due to the presence of an explosophoric group 1-amino-2,2-dinitroethylene or dinitromethane. Compounds **5c**, **9**, and **12b** are insensitive compared with the other 1-amino-2,2-dinitroethylene or dinitromethane derivatives (Table 1).

Further, the stability and sensitivity properties are predicted using the Hirshfeld surfaces and 2D fingerprint analysis for crystals of **11**, **12a** and compared with experimental thermostabilities and mechanical sensitivities (Fig. 8).²⁶ In the Hirshfeld surfaces analysis, the red and blue dots indicate high and low intermolecular interactions through the surrounding molecule's external atoms (H, N and O). high and low intermolecular interactions through the external atoms (H, N and O) surrounding molecule. In 2D fingerprint plots, the spikes indicate the strong O...H and N...H interactions. There is a significant contribution of hydrogen bond interactions in both compounds, while in **11** effective N–O (18.7%) and N–N (11.8%), which results as sensitive compared with compound **12a**.

Conclusion

In summary, we have studied the selective reactivity of HFOX with various carbonyl derivatives under acidic and basic conditions. The HFOX resonance intermediates play a major role on the product outcome. With the protonated form of HFOX (i), only the hydrazinyl group participates in the condensation reactions with carbonyl compounds. Whereas in the case of the anionic form of HFOX (ii), both amine and hydrazinyl groups participate in these reactions. All the new compounds are comprehensively characterized by advanced spectroscopic techniques, and the structures of **5**, **5c**, **5e**, **9**, **11**, and **12a** were analyzed by single crystal X-ray analysis. The crystal structures of potassium (**5**) and sodium (**5e**) triazine salts were found to be three-dimensional energetic metal-organic frameworks (3D EMOFs). Thermostabilities and mechanical sensitivities are measured, many of the triazine salts are highly stable and less sensitive to impact and friction. All these new compounds are energetic, and all the detonation properties were calculated by using EXPLO5 (version 6.01). Most new compounds exhibit good detonation performance, superior to that of TNT. Overall, the synthetic strategy provides a valuable and efficient route for the selected synthesis of high-performing and insensitive FOX-7 derivatives.

Data availability

Details of experimental procedures, characterizations, theoretical calculations, X-ray crystal diffraction data and crystal

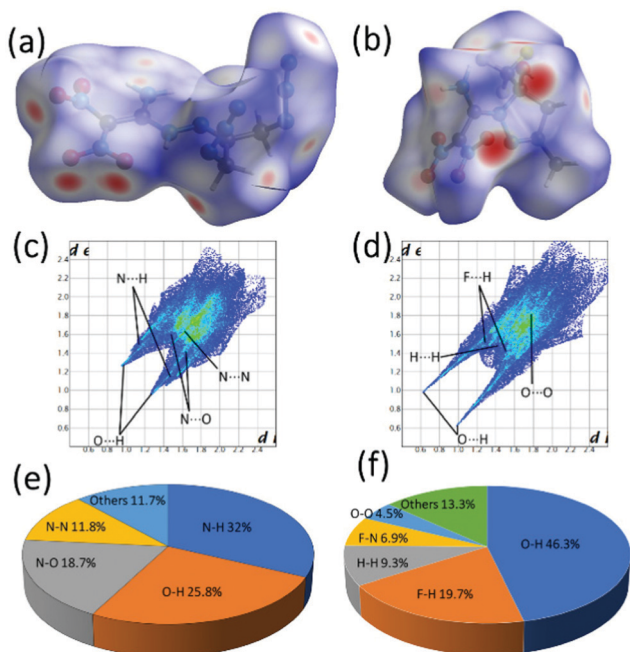


Fig. 8 (a) and (b) Hirshfeld surfaces of **11** and **12a**. (c) and (d) Fingerprint plots of **11** and **12a**. (e) and (f) The percentage of atomic contact contributions in **11** and **12a**.



structures for compounds **5**, **5c**, **5e**, **9**, **11**, **12a**, and NMR spectra are provided in the ESI.†

Author contributions

A. K. C. investigation, methodology, and manuscript writing. R. J. S. X-ray data collection and solved the structures. A. K. C. and J. M. S. conceptualisation, manuscript writing – review and editing, supervision.

Conflicts of interest

There are no conflicts to declare.

Acknowledgements

The Rigaku Synergy S Diffractometer was purchased with support from the National Science Foundation MRI program under Grant No. 1919565.

Notes and references

- 1 A. J. Bellamy, *FOX-7 (1,1-diamino-2,2-dinitroethene). Struct. Bonding, High Energy Density Materials*, Berlin, Ger., 2007, vol. 125, pp. 1–33.
- 2 (a) N. V. Latypov, J. Bergman, A. Langlet, U. Wellmar and U. Bemm, *Tetrahedron*, 1998, **54**, 11525–11536; (b) U. Bemm and H. Ostmark, *Acta Crystallogr.*, 1998, **C54**, 1997–1999.
- 3 G. Herve, G. Jacob and N. Latypov, *Tetrahedron*, 2005, **61**, 6743–6748.
- 4 H. Gao and J. M. Shreeve, *RSC Adv.*, 2016, **6**, 56271–56277.
- 5 C. Yan, H. Yang, X. Qi, Y. Jin, K. Wang, T. Liu, J. Tian, F. Nie, G. Cheng and Q. Zhang, *Chem. Commun.*, 2018, **54**, 9333–9336.
- 6 (a) A. J. Bellamy, N. V. Latypov and P. Goede, *J. Chem. Res., Synop.*, 2002, 257; (b) A. J. Bellamy, A. E. Contini and N. V. Latypov, *Propellants, Explos., Pyrotech.*, 2008, **33**, 87–88.
- 7 T. T. Vo and J. M. Shreeve, *J. Mater. Chem. A*, 2015, **3**, 8756–8763.
- 8 Q. J. Axthammer, B. Krumm and T. M. Klapötke, *J. Phys. Chem. A*, 2017, **121**, 3567–3579.
- 9 A. R. Katritzky, G. L. Sommen, A. V. Gromova, R. M. Witek, P. J. Steel and R. Damavarapu, *Chem. Heterocycl. Compd.*, 2005, **41**, 111–118.
- 10 Q. Qiu, X. Yang, K. Xu, Z. Gao, J. Song, S. Yang and F. Zhao, *Inorg. Chim. Acta*, 2013, **405**, 356–361.
- 11 T. Zhou, X. Guan, K. Xu, J. Song and F. Zhao, *Chem. Heterocycl. Compd.*, 2017, **53**, 710–713.
- 12 H. Gao, Y.-H. Joo, D. A. Parrish, T. T. Vo and J. M. Shreeve, *Chem. – Eur. J.*, 2011, **17**(16), 4613–4618.
- 13 T. T. Vo, D. A. Parrish and J. M. Shreeve, *Inorg. Chem.*, 2012, **51**, 1963–1968.
- 14 T. T. Vo, J. Zhang, D. A. Parrish, B. Twamley and J. M. Shreeve, *J. Am. Chem. Soc.*, 2013, **135**, 11787–11790.
- 15 S. Dharavath, L. A. Mitchell, D. A. Parrish and J. M. Shreeve, *Chem. Commun.*, 2016, **52**, 7668–7671.
- 16 T. T. Vo, D. A. Parrish and J. M. Shreeve, *J. Am. Chem. Soc.*, 2014, **136**, 11934–11937.
- 17 H. Gao and J. M. Shreeve, *Angew. Chem.*, 2015, **127**, 6433–6436 (*Angew. Chem., Int. Ed.*, 2015, **54**, 6335–6338).
- 18 J. Zhang, S. Dharavath, L. A. Mitchell, D. A. Parrish and J. M. Shreeve, *J. Am. Chem. Soc.*, 2016, **138**, 7500–7503.
- 19 S. Dharavath, J. Zhang, G. H. Imler, D. A. Parrish and J. M. Shreeve, *J. Mater. Chem. A*, 2017, **5**, 4785–4790.
- 20 S. Dharavath, Y. Tang, D. Kumar, L. A. Mitchell, D. A. Parrish and J. M. Shreeve, *Eur. J. Org. Chem.*, 2019, 3142–3145.
- 21 A. K. Chinnam, R. J. Staples and J. M. Shreeve, *Org. Lett.*, 2021, **23**, 76–80.
- 22 A. Astrat'ev, D. Dashko and A. Stepanov, *New Trends Res. Energ. Mater., Proc. Semin., 14th*, 2011, **2**, 469–481.
- 23 M. J. Frisch, G. W. Trucks, H. B. Schlegel, G. E. Scuseria, M. A. Robb, J. R. Cheeseman, J. A. Montgomery Jr., T. Vreven, K. N. Kudin, J. C. Burant, J. M. Millam, S. S. Iyengar, J. Tomasi, V. Barone, B. Mennucci, M. Cossi, G. Scalmani, N. Rega, G. A. Petersson, H. Nakatsuji, M. Hada, M. Ehara, K. Toyota, R. Fukuda, J. Hasegawa, M. Ishida, T. Nakajima, Y. Honda, O. Kitao, H. Nakai, M. Klene, X. Li, J. E. Knox, H. P. Hratchian, J. B. Cross, V. Bakken, C. Adamo, J. Jaramillo, R. Gomperts, R. E. Stratmann, O. Yazyev, A. J. Austin, R. Cammi, C. Pomelli, J. W. Ochterski, P. Y. Ayala, K. Morokuma, G. A. Voth, P. Salvador, J. J. Dannenberg, V. G. Zakrzewski, S. Dapprich, A. D. Daniels, M. C. Strain, O. Farkas, D. K. Malick, A. D. Rabuck, K. Raghavachari, J. B. Foresman, J. V. Ortiz, Q. Cui, A. G. Baboul, S. Clifford, J. Cioslowski, B. B. Stefanov, G. Liu, A. Liashenko, P. Piskorz, I. Komaromi, R. L. Martin, D. J. Fox, T. Keith, M. A. Al-Laham, C. Y. Peng, A. Nanayakkara, M. Challacombe, P. M. W. Gill, B. Johnson, W. Chen, M. W. Wong, C. Gonzalez and J. A. Pople, *Gaussian 03 (Revision E.01)*, Gaussian, Inc., Wallingford CT, 2004.
- 24 M. Sućeska, *EXPLO5 6.01*, Brodarski Institute, Zagreb, Croatia, 2013.
- 25 (a) A 20 mg sample was subjected to a drop-hammer test with a 5 or 10 kg dropping weight. The impact sensitivities were characterized according to the UN recommendations (insensitive, > 40 J; less sensitive, 35 J; sensitive, 4 J; very sensitive, 3 J); (b) *United Nations Recommendations on the Transport of Dangerous Goods. Manual of Tests and Criteria*, United Nations Publication, New York, 2009.
- 26 M. J. Turner, J. J. M. McKinnon, S. K. Wolff, D. J. Grimwood, P. R. Spackman, D. Jayatilaka and M. A. Spackman, *Crystal Explorer 17*, University of Western Australia, 2017.

